

East Model: Basis Set Expansion, Mode Coupling, and Irreducible Memory Kernels[†]

Jianlan Wu and Jianshu Cao*

Department of Chemistry, Massachusetts Institute of Technology, Cambridge, Massachusetts 02139

Received: November 24, 2003; In Final Form: February 24, 2004

A matrix formalism defined in the complete dynamic phase space is developed to analyze spin relaxation in the East model and the dynamic slow-down of dissipative systems in general. The truncated basis set expansion provides a direct route to calculate spin correlation functions systematically and to evaluate the mean relaxation time. Examining the relaxation time scales of linear and nonlinear modes leads to the observation that the *full correlation* and *irreducible correlation* functions defined in the *complete space* describe the slow dynamics of a dissipative system and can be related to their equivalent physical quantities in nondissipative systems, whereas the *reduced correlation* functions and associated memory kernels defined in the *projected space* involve faster time scales and cannot be directly reduced through mode coupling approximations. Matrix relations allow us to recover the simple mode coupling and extended mode coupling equations first obtained through an elegant diagrammatic expansion by Pitts and Anderson (*J. Chem. Phys.* **2001**, *114*, 1101). These mode coupling approaches are extended to low temperatures by analyzing higher order nonlinear modes and correcting mode coupling closures with the asymptotic behavior. Further, the second-order full correlation function can be clearly separated into the short time regime evaluated by basis set expansion and the long-time regime described by a stretched exponential arising from domain dynamics, and the resulting single-spin self-correlation function agrees with simulations over the whole temporal range.

I. Introduction

The dynamics of glass-forming liquids is a challenging problem, which requires a transparent and unified theoretical framework. Motivated by this challenge, Fredrickson and Anderson (FA) proposed a kinetic Ising model, where spin dynamics is controlled by local kinetic constraints instead of many-body interaction potentials.^{1,2} The FA model can be viewed as a physical realization of the hierarchically constrained mechanism suggested by Abrahams et al.³ and exhibits cooperative motions often described by the thermal-statistical theory of glass transitions developed by Adams and Gibbs⁴ and by Wolynes and co-workers.^{5,6} Jackle and co-workers extended the FA model to a large class of kinetically constrained models (KCM), including the East model,^{7,8} which is the focus of this article. A key question one hopes to address with this type of models is: Can the glass transition be understood from the perspective of purely kinetic constraints without an underlying thermodynamic transition? This question has inspired extensive discussions. For example, Garrahan and Chandler explored the spatial-temporal structures of domain dynamics in the KCMs using the intriguing concept of trajectory statistics.^{9,10} However, we will not discuss this question in this article; instead, we are interested in another possibility: Given the simplicity of these models (e.g., the East model), can we achieve a better understanding of existing theoretical tools for describing viscous dynamics? To address this possibility, we develop a matrix formalism based on the complete basis set of the East model and use it to investigate the assumptions, limitations, and possible extensions of the standard theoretical techniques, e.g., mode coupling theory (MCT).

The East model is a one-dimensional (1D) spin chain where each spin is only allowed to flip if the next spin on the right is in the up state. The concentration of up-spins is given by a constant c , which is related to temperature by $c = 1/(1 + e^{1/T})$. Among various approaches developed to study this model, the most relevant to our work is the asymptotic relations and mode coupling closures. Jackle and Eisinger used the effective-medium approximation (EMA) and the cluster expansion method (CEM) to calculate response functions.⁸ Mauch and Jackle extended CEM and found that the mean relaxation time increases as $\tau_1 \sim \mathcal{O}(c^{\log_2 c})$ in the small c limit.¹¹ Sollich and Evans explained this result by analyzing domains composed of down-spins between two adjacent up-spins.^{12–15} Aldous and Diaconis provided a rigorous mathematical proof of this asymptotic result.¹⁶ These known asymptotic relations and the high-order mode coupling trees (as shown in Figure 1) make the East model a unique and attractive choice for systematically studying the dynamic slow-down at low temperatures (i.e., small c values).

Along a different line, MCT has been applied to the single-spin self-correlation function $C_1(t)$ of the East model. Jackle was the first to evaluate the memory kernel $M_1(t)$ by a Gaussian factorization scheme: $M(t) \propto C_1^2(t)$.⁸ The prediction from this approximation is not satisfactory when compared with simulations. Kawasaki proposed that the mode coupling (MC) approximation should be applied to the irreducible memory kernel $M_1^{\text{ir}}(t)$, which is a polynomial of $C_1(t)$.¹⁸ Pitts and Anderson developed an elegant diagrammatic theory for KCMs and obtained the irreducible memory kernel from a set of irreducible diagrams.^{19,20} A subset of these irreducible diagrams leads to the simple mode coupling approximation (SMC) for the East model: $M_1^{\text{ir}}(t) \approx c(1 - c)C_1(t)$. The resulting correlation function is reliable for $c > 0.5$ but does not decay to zero for

[†] Part of the special issue "Hans C. Andersen Festschrift".

* Corresponding author. E-mail: jianshu@mit.edu.

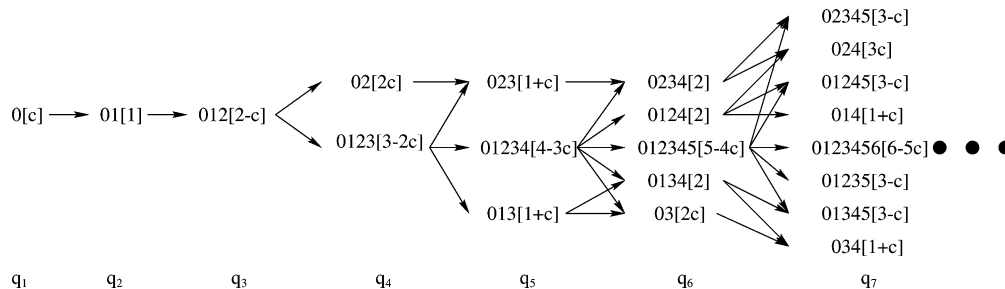


Figure 1. MC tree for sorting the complete basis set and visualizing mode-couplings, where all the modes up to q_7 are displayed.

$c < 0.5$ ($T_c = \infty$). It is known that the East model does not have a glass transition at a nonzero temperature and exhibits a divergent time scale only at $c = 0$ (i.e., $T_g = 0$). To avoid the unphysical ergodic-to-nonergodic transition, Pitts and Anderson extended SMC to the extended mode coupling (EMC) by incorporating higher order diagrams through a difference function $\Delta(z)$. The prediction of EMC removes the plateau but decays too fast for $c \leq 0.5$. A central result of this article is to derive SMC and EMC through matrix algebra and improve the accuracy of our prediction in the temperature regime between T_c and T_g through the use of the asymptotic relations and better mode coupling closures. In many ways, Anderson's diagrammatic theory inspired our theoretical efforts. An interesting outcome is the equivalence between the two formalisms for the East model, as demonstrated in Figure 5.

The matrix formalism and conclusions drawn from our analysis are not limited to the East model and are completely general for a class of dissipative systems with detailed balance, such as colloids and lattice spin models.^{21,22} In their study of interacting Brownian particles, Cichocki and Hess found that the memory function for density fluctuations of colloids cannot be interpreted as a generalized dynamic viscosity and is not a good candidate for MC approximations. Instead, they introduced an irreducible memory kernel, which is related to the memory kernel and displays the characteristics of dynamic viscosity.²³ Kawasaki introduced a rigorous operator definition of the irreducible memory kernel.¹⁸ An important physical insight was observed by Pitts and Anderson via comparing the dynamic structures of dissipative and nondissipative systems.²⁴ Their analysis revealed that the irreducible memory function, rather than the second-order memory function, has a more fundamental physical interpretation and is more useful for constructing mode coupling theories. Our matrix formalism provides an alternative perspective on the issue of the irreducible memory kernels and introduces a class of full and irreducible correlation functions that are slow functions and a class of reducible memory kernels and correlation functions that are fast functions. This formal development is presented in section IV and Appendices B and C. Readers who are mainly interested in the detailed calculations of the East model can skip the formal analysis.

Outline of the Article. Through the analysis of the East model, we investigate the nature of the irreducible memory kernel and collective kinetics in the temperature regime between T_g and T_c . The starting point of our calculations is the construction of the complete basis set in section II.^{20,25,26} The truncated basis set expansion represented symbolically by the mode coupling tree in section III is a direct and systematic method to calculate the single-spin self-correlation function. In section IV, this technique combined with the small- c asymptotics allows us to calculate the mean relaxation times of linear and nonlinear spin correlation functions, as well as their relationships. As a general result, we find that *the complete dynamic phase space including all the relevant dynamic modes rather*

than any subspace where one or more relevant modes are projected out is required in describing slow dynamics of dissipative systems. As a result, full correlation functions $C_k(t)$ and irreducible correlation functions $C_k^{\text{ir}}(t)$ defined in the complete space are slow functions, whereas reduced correlation functions $C_k^{\text{r}}(t)$ and standard memory kernels $M_k(t)$ defined in projected space are not necessarily slow. MC closures or long-time asymptotic relations must be applied to $C_k^{\text{ir}}(t)$ and $C_k(t)$, which are related through a simple identity. The matrix derivation in Appendix B obtains recursive expressions for $C_k(t)$ and $C_k^{\text{ir}}(t)$. The equivalence to Kawasaki's operator definition of $M_1^{\text{ir}}(t)$ ¹⁸ is shown in Appendix C and is generalized to higher orders.

Next we study collective kinetics by MC closures. Linear relations between $C_1(t)$ and $C_k^{\text{ir}}(t)$ allow us to recover Pitts and Andersen's SMC^{19,20} and its higher order generalization in section V. To remove the plateau predicted by SMC closures, we calculate perturbatively a difference function $\Delta(z)$ between the exact $\hat{M}_1^{\text{ir}}(z)$ and the SMC closure in section VIA, resulting in the EMC formulation proposed by Pitts and Andersen.²⁰ From accurate long-time asymptotic relationships, we derive a long-time correction method, which agrees with the simulation for small c in section VIB. However, all these microscopic methods can only describe cooperative motions in a limited temporal range and are not applicable near the divergence point.

In section VIII, we discuss the stretched exponential functional form in the East model. The stretched exponential form predicted by domain dynamics is found to fit $C_1(t)$ in a limited temporal range.^{14,15,19,33} From the simulations, we find that the two-spin correlation function $C_2(t)$ can be clearly separated into a short-time regime described by the basis set perturbation and a long-time regime fitted by a stretched exponential form. As a convolution of $C_2(t)$, the approximation to $C_1(t)$ agrees with simulations over the whole temporal range. This result supports indirectly the notation of domain dynamics and suggests that it is a better approach to describe slow relaxations in the East model.

II. Complete Basis Set of the East Model

We present a brief introduction of the East model in this section.^{7,8} The complete basis set of this model is constructed following the general approach by Oppenheim et al.^{25,26} and is the fluctuation basis defined by Pitts and Anderson.^{19,20} Corresponding to the adjoint kinetic operator \mathbf{L} , a matrix \mathbf{L} is defined to describe kinetics of all the modes in the complete basis set.²⁶

The East model is a 1D chain of spins that can have two values, $n_i = 1, 0$.^{7,8} A spin at position i can change the value of n_i only if its nearest neighbor on the right, spin $i + 1$, is in the upstate, $n_{i+1} = 1$. The corresponding rate constants are $k_{0 \rightarrow 1} = c$ and $k_{1 \rightarrow 0} = 1 - c$. Satisfying the detailed balance gives the average concentration c of up-spins ($n_i = 1$), which is related

to the temperature by $c = 1/(1 + e^{1/T})$ for $0 \leq c \leq 1/2$. A general rate equation is⁸

$$\dot{n}_i = \mathbf{L}n_i = -n_{i+1}\Delta n_i \quad (1)$$

where Δn_i is the occupation fluctuation, $\Delta n_i = n_i - c$. The equilibrium distribution of the system is trivial, $f_{\text{eq}}(n_i = 1) = c$ and $f_{\text{eq}}(n_i = 0) = 1 - c$. The correlation function of a dynamic variable A is defined as $C_A(t) \equiv \langle f_{\text{eq}} A e^{\mathbf{L}t} A \rangle$, where the angular bracket is a direct average over phase space Γ , $\langle A(\Gamma) \rangle = \int d\Gamma A(\Gamma) / \int d\Gamma$, and f_{eq} is on the left side as a result of using the adjoint kinetic operator \mathbf{L} .^{8,23}

By distinguishing linear and nonlinear modes as slow and fast modes, and applying the Markovian approximation to fast modes, we can reliably predict relaxations in gas and normal liquids. In glass-forming liquids, non-Markovian processes dominate and nonlinear modes become slow and have to be categorized by their characteristic relaxation time scales. Following this idea, we include all the products of relevant linear modes in a complete basis set Γ . The value of each dynamic variable at any given time is a linear combination of projections onto all the modes, consistent with the Mori continued fraction method.²⁷ In this article, the complete basis set is the starting point of our theoretical analysis. In practice, the construction of the complete basis set is associated with the Gram–Schmidt orthonormalization method.^{20,25,26} The linear mode in the East model, $A_1(i)$, corresponds to the fluctuation of spin i and is given by⁸

$$A_1(i) = \frac{\Delta n_i}{\sqrt{c(1-c)}} \quad (2)$$

which satisfies $\langle f_{\text{eq}} A_1(i) \rangle = 0$ and $\langle f_{\text{eq}} A_1(i) A_1(i') \rangle = \delta_{i,i'}$ where δ is the Kronecker delta function. Nonlinear modes are generated from different spins because of the identity $n^s \equiv n$ ($s > 0$). Each m th-order ($m \geq 1$) nonlinear mode factorizes as

$$A_m(i_1 i_2 \cdots i_m) = A_1(i_1) A_1(i_2) \cdots A_1(i_m) \quad (3)$$

where the indexes are ordered as ($i_1 < i_2 < \dots < i_m$) to avoid overcounting. Because each mode is a unique function of its sequence, ($i_1 i_2 \cdots i_m$) represents mode A_m unambiguously. All the modes in this complete basis set are orthonormal, $\langle f_{\text{eq}} A_m A_{m'} \rangle = \delta_{m,m'}$.

We expand the adjoint kinetic operator \mathbf{L} in this complete basis set to construct a matrix \mathbf{L} by defining $L_{m,m'} \equiv \langle f_{\text{eq}} A_m \mathbf{L} A_{m'} \rangle$. We prove in Appendix A that the diagonal matrix element $L_{m,m}$ is

$$\begin{aligned} L_{m,m} &= \langle f_{\text{eq}} A_m(i_1 i_2 \cdots i_m) \mathbf{L} A_m(i_1 i_2 \cdots i_m) \rangle \\ &= -[(m-p)c + p(1-c)] \end{aligned} \quad (4)$$

where p is the number of spins that satisfy $i_{[k+1]} = i_k + 1$. Off-diagonal elements are nonzero for the coupling between A_m and modes in the set $\{A_{m'}\}$, which is

$$A_{m'} = \begin{cases} A_{m-1}(i_1 i_2 \cdots i_k i_{[k+2]} \cdots i_m) & \text{if } i_{[k+1]} = i_k + 1 \\ A_{m+1}(i_1 i_2 \cdots i_k [i_k + 1] i_{[k+1]} \cdots i_m) & \text{if } i_{[k+1]} > i_k + 1 \end{cases} \quad (5)$$

and all the nonzero off-diagonal matrix elements have the same value,

$$L_{m,m'} = \langle f_{\text{eq}} A_m \mathbf{L} A_{m'} \rangle = -\sqrt{c(1-c)} \quad (6)$$

We denote the space composed of the modes with the same first spin i as Γ_i . Because each mode in the space Γ_i is only influenced by other modes in Γ_i , Γ_i is an independent closed subspace of Γ . Our future derivations are restricted to Γ_0 , which will be considered the complete space (basis set) in the remainder of this article.

III. Basis Set Expansion

The structure of matrix \mathbf{L} implies that there is no cross correlation function between different spins in the East model: $C_1(i, j; t) \equiv \langle f_{\text{eq}} A_1(i) e^{\mathbf{L}t} A_1(j) \rangle = C_1(t) \delta_{i,j}$, where $C_1(t)$ is the single-spin self-correlation function. As the first step of our theoretical analysis, we apply a basis set expansion method to calculate $C_1(t) = \langle f_{\text{eq}} A_1(0) e^{\mathbf{L}t} A_1(0) \rangle$.

For convenience, we sort all the modes in Γ_0 into basis sets of different orders, denoted by q_k where the order index is k . Note that k refers to a set, whereas m refers to a single mode. Beginning with the first-order basis set $q_1 = \{A_1(0)\}$, each subsequent ($k+1$)th-order basis set q_{k+1} is composed of modes that are coupled to one or more modes in the k th-order basis set q_k . Each kinetic block matrix satisfies

$$L_{k,k'} \equiv \langle f_{\text{eq}} q_k \mathbf{L} q_{k'} \rangle = L_{k,k\pm 1} \delta_{k',k\pm 1} + L_{k,k} \delta_{k',k} \quad (7)$$

As shown in Figure 1, the first four basis sets are $q_1 = \{A_1(0)\}$, $q_2 = \{A_2(01)\}$, $q_3 = \{A_3(012)\}$, $q_4 = \{A_2(02), A_4(0123)\}$. The kinetic matrix \mathbf{L} becomes a block tridiagonal matrix after sorting.

To visualize \mathbf{L} , we introduce the *MC tree* shown in Figure 1. Numbers preceding a bracket denote the spin sequence of a mode, and the number inside the bracket denotes the eigenfrequency Ω of this mode, i.e., negative of the corresponding diagonal matrix element of \mathbf{L} . For example, $0[c]$ represents $A_1(0)$ with $\Omega_1 = c$, and $01[1]$ represents $A_2(01)$ with $\Omega_2 = 1$. The modes in the same column belong to a basis set of the same order. Each arrow represents a nonzero kinetic coupling by eq 6 between the two modes connected by this arrow, corresponding to off-diagonal block matrices $L_{k,k+1}$ and $L_{k+1,k}$. For example, arrows between $q_4 = \{A_2(02), A_4(0123)\}$ and $q_5 = \{A_3(023), A_5(01234), A_3(013)\}$ give

$$\begin{aligned} L_{4,5} &= -\sqrt{c(1-c)} \begin{bmatrix} 1 & 0 & 0 \\ 1 & 1 & 1 \end{bmatrix} \\ L_{5,4} &= -\sqrt{c(1-c)} \begin{bmatrix} 1 & 1 \\ 0 & 1 \\ 0 & 1 \end{bmatrix} \end{aligned} \quad (8)$$

Because the Laplace transform of $C_1(t)$ is $\hat{C}_1(z) = \langle f_{\text{eq}} q_1 (z\mathbf{I} - \mathbf{L})^{-1} q_1 \rangle$, the calculation of $C_1(t)$ is equivalent to inverting the matrix,

$$z\mathbf{I} - \mathbf{L} = \begin{bmatrix} z\mathbf{I} - L_{1,1} & -L_{1,2} & & \\ -L_{2,1} & z\mathbf{I} - L_{2,2} & \ddots & \\ & \ddots & \ddots & \ddots \\ & & & z\mathbf{I} - L_{n,n} \end{bmatrix} \quad (9)$$

where each block matrix is defined by eq 7, \mathbf{I} is the identity operator, and \mathbf{I} is the identity matrix. Applying block matrix decompositions, $\hat{C}_1(z)$ becomes

$$\begin{aligned} \hat{C}_1(z) &= [(z\mathbf{I} - \mathbf{L})^{-1}]_{1,1} = [z + \Omega_1 - \hat{M}_1(z)]^{-1} \\ &= [z - L_{1,1} - L_{1,2} \hat{C}_2^t(z) L_{2,1}]^{-1} \end{aligned} \quad (10)$$

where Ω_1 is the first-order eigenfrequency, $\hat{M}_1(z)$ is the first-order memory kernel, and $\hat{C}_2^t(z) = [(z\mathbf{I} - L_2^t)^{-1}]_{1,1}$ is defined

by a submatrix,

$$\mathbf{L}_2^r = \begin{bmatrix} \mathbf{L}_{2,2} & \mathbf{L}_{2,3} & & \\ \mathbf{L}_{3,2} & \mathbf{L}_{3,3} & \ddots & \\ & \ddots & \ddots & \ddots \\ & & \ddots & \ddots \end{bmatrix} \quad (11)$$

Extending the decomposition to higher orders results in the k th-order *reduced correlation function*, $\hat{C}_k^r(z) \equiv [(z\mathbf{I} - \mathbf{L}_k^r)^{-1}]_{1,1}$, where

$$\mathbf{L}_k^r = \begin{bmatrix} \mathbf{L}_{k,k} & \mathbf{L}_{k,k+1} & & \\ \mathbf{L}_{k+1,k} & \mathbf{L}_{k+1,k+1} & \ddots & \\ & \ddots & \ddots & \ddots \\ & & \ddots & \ddots \end{bmatrix} \quad (12)$$

By removing all the modes on the left side of q_k in Figure 1, we get the MC tree corresponding to \mathbf{L}_k^r . Similar to eq 10, we have a recursive equation for $\hat{C}_k^r(z)$,

$$\hat{C}_k^r(z) = [z\mathbf{I} + \mathbf{\Omega}_k - \hat{\mathbf{M}}_k(z)]^{-1} \quad (13)$$

where the k th-order eigenfrequency matrix is $\mathbf{\Omega}_k = -\mathbf{L}_{k,k}$ and the k th-order memory kernel is $\hat{\mathbf{M}}_k(z) = \mathbf{L}_{k,k+1}\hat{C}_{k+1}^r(z)\mathbf{L}_{k+1,k}$. By definition, $C_k^r(t)$ differs from the *full correlation function* $C_k(t)$, where all the modes in Γ_0 are taken into account, $C_k(t) \equiv \langle f_{\text{eq}} q_k e^{\mathbf{L}t} q_k \rangle$. The recursive expression for full correlation functions is derived in Appendix B. These two correlation functions are employed to study relaxations of nonlinear modes in the next section.

Motivated by standard truncation techniques, we apply a basis set expansion method, which is equivalent to the Mori continued fraction formalism.²⁷ Truncated at the first-order basis set q_1 , we have $z\mathbf{I} - \mathbf{L} \approx z\mathbf{I} - \mathbf{L}_{1,1} = z + c$ and $\hat{C}_1^{(1)}(z) = (z + c)^{-1}$. Truncated at q_2 , we have

$$z\mathbf{I} - \mathbf{L} \approx \begin{bmatrix} z\mathbf{I} - \mathbf{L}_{1,1} & -\mathbf{L}_{1,2} \\ -\mathbf{L}_{2,1} & z\mathbf{I} - \mathbf{L}_{2,2} \end{bmatrix} = \begin{bmatrix} z + c & \sqrt{c(1-c)} \\ \sqrt{c(1-c)} & z + 1 \end{bmatrix} \quad (14)$$

and $\hat{C}_1^{(2)}(z) = [z + c - c(1-c)(z+1)^{-1}]^{-1}$. In general, truncation at q_k ignores all the modes higher than q_k . As a result, we approximate the matrix $(z\mathbf{I} - \mathbf{L})$ as

$$z\mathbf{I} - \mathbf{L} \approx \begin{bmatrix} z\mathbf{I} - \mathbf{L}_{1,1} & -\mathbf{L}_{1,2} & & & \\ -\mathbf{L}_{2,1} & \ddots & \ddots & & \\ & \ddots & \ddots & \ddots & \\ & & \ddots & \ddots & -\mathbf{L}_{k-1,k} \\ & & & -\mathbf{L}_{k,k-1} & z\mathbf{I} - \mathbf{L}_{k,k} \end{bmatrix} \quad (15)$$

and the k th-order basis set expansion of the single-spin self-correlation function becomes

$$\hat{C}_1^{(k)}(z) = 1/z + c - c(1-c)/z + 1 - c(1-c)/z + 2 - c - \dots/z + \mathbf{\Omega}_k \quad (16)$$

where matrix manipulations are implicit.

By plotting $C_1^{(3)}(t)$, $C_1^{(6)}(t)$ and simulations in Figure 2, we find that with the increase of expansion order, the accuracy of the theoretical predictions systematically increases. For a large c (0.8), the truncation at q_3 already provides a reliable prediction of $C_1(t)$. As c decreases, the minimum truncation order to reliably predict $C_1(t)$ is around c^{-1} , which implies that the expansion method is not practical near the divergence point, $c_g = 0$ ($T_g = 0$). In fact, $C_1^{(k)}(t)$ predicted from the truncation

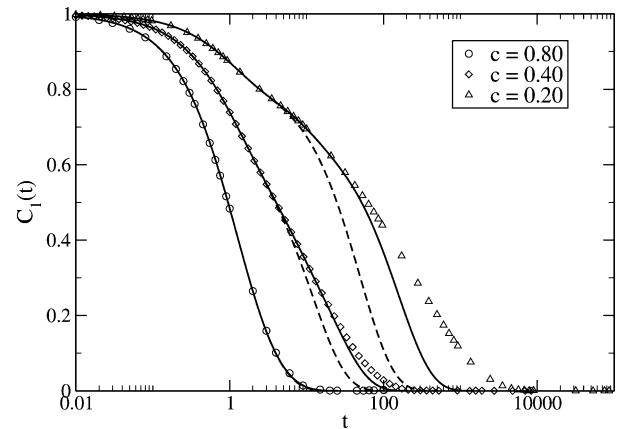


Figure 2. Comparison of $C_1(t)$ from basis set expansions and from simulations for $c = 0.2, 0.4$, and 0.8 . The dashed lines are $C_1^{(3)}(t)$ truncated at $q_3 = \{A_3(012)\}$. The solid lines are $C_1^{(6)}(t)$ truncated at $q_6 = \{A_2(03), A_4(0124), A_4(0134), A_4(0234), A_6(012345)\}$. The symbols are simulation results.

technique is a multiexponential function of t . Heterogeneous cooperative motions suggest that $C_1(t)$ follows a more complicated form as demonstrated by Pitts, Young and Andersen.¹⁹

IV. Mean Relaxation Time and Slow Dynamics of Nonlinear Modes

Because of the truncation at a finite order, the finite basis set expansion method cannot fully account for many-body effects, and the predictions of $C_1(t)$ deviate from simulations in the long-time limit. Using non-Markovian approximations such as MC closures, kinetics of nonlinear modes is expected to help improve predictions of $C_1(t)$. For dissipative systems, MC is applied to the irreducible memory kernel $\mathbf{M}_1^{\text{ir}}(t)$ rather than $\mathbf{M}_1(t)$. Although several explanations of $\mathbf{M}_1^{\text{ir}}(t)$ were proposed in the literatures,^{23,24} and a generalized operator formalism was developed by Kawasaki,¹⁸ our basis set formalism provides an alternative perspective. On the basis of the analysis of the East model, which is a simple dissipative system with established asymptotics,^{9,11-16} we demonstrate the preference of $\mathbf{M}_1^{\text{ir}}(t)$ to $\mathbf{M}_1(t)$ in the MC closure from the view of the complete basis set.

A. Lowest MC Tree. The mean relaxation time of the linear mode is defined as $\tau_1 \equiv \int_0^\infty dt C_1(t) = \hat{C}_1(0)$, which can be evaluated by the basis set expansion. Following Mauch and Jackle's approach,¹¹ we attempt to achieve the dynamic scaling by calculating $\tau_1(N)$ for a finite N -spin chain beginning with spin 0. Imposed by a fixed boundary condition, $n_N(t) = 1$, we have $\tau_1(1) = c^{-1}$ for a one-spin chain, and

$$\begin{aligned} \tau_1(2) &= (\mathbf{\Omega}_1 - \mathbf{L}_{1,2}\mathbf{\Omega}_2^{-1}\mathbf{L}_{2,1})^{-1} \\ &= [c - c(1-c)]^{-1} = c^{-2} \end{aligned} \quad (17)$$

for a two-spin chain. To facilitate calculations of $\tau(N)$, we apply the MC tree introduced in section III to finite spin chains. Because only spin i ($0 \leq i < N$) is involved in the N -spin chain, a new finite MC tree for this chain is constructed by excluding all the modes with spin j ($j \geq N$). Note that a truncation at spin N is different from the truncation at q_k for $C_1^{(k)}(t)$. As a result, the highest order reduced correlation function is $\hat{C}_K^r(z) = (z\mathbf{I} + \mathbf{\Omega}_K)^{-1}$, where K denotes the highest order basis set in the new MC tree. All the lower order functions are then recursively

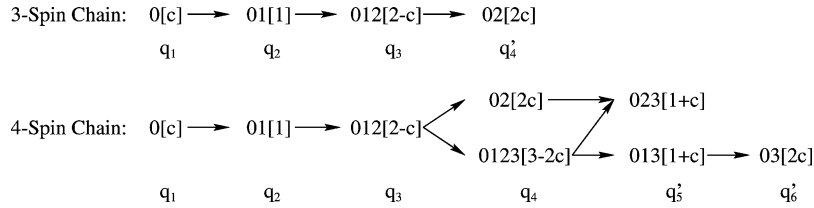


Figure 3. MC trees for three-spin and four-spin chains. As a result of truncation at spin 2 and spin 3, q_4' in the three-spin chain and q_5' and q_6' in the four-spin chain differ from their counterparts in Figure 1.

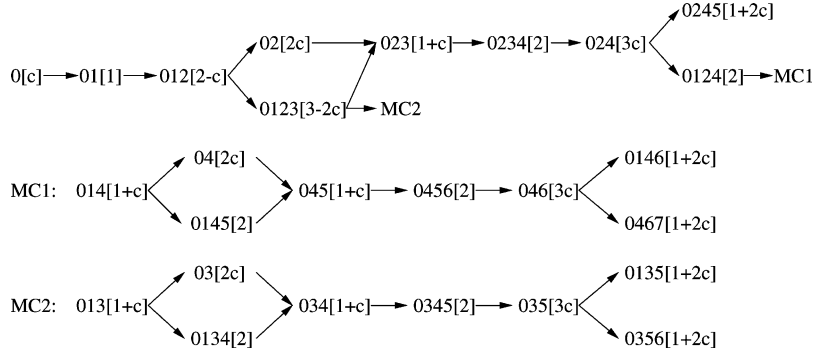


Figure 4. Truncated at spin 7, the lowest MC tree for an eight-spin chain, where labels of basis sets are omitted. The number of spins for each mode is smaller than or equal to 4 ($1 + \log_2 8$).

obtained, e.g., $\hat{C}_2^r(z) = (z + 1)^{-1}$ and $\tau_1(2) = c^{-2}$ for the two-spin chain. The MC trees for three-spin and four-spin chains are shown in Figure 3, giving $\tau_1(3) \xrightarrow{c \rightarrow 0} \mathcal{O}(c^{-2})$ and $\tau_1(4) \xrightarrow{c \rightarrow 0} \mathcal{O}(c^{-3})$.

Similar to Mauch and Jackle's calculations,¹¹ we find that modes in a finite MC tree contribute to τ_1 at different orders of c . For example, for the four-spin chain, the lowest MC tree,

$$0[c] \rightarrow 01[1] \rightarrow 012[2 - c] \rightarrow 02[2c] \rightarrow 023[1 + c]$$

provides the leading term, $\tau_1(4) \sim \mathcal{O}(c^{-3})$, whereas a branch,

$$0123[3 - 2c] \rightarrow 013[1 + c] \rightarrow 03[2c]$$

only helps modify the coefficient of c^{-3} . By extrapolating results for $N(\leq 16)$ -spin chains, we find that $\tau_1(N)$ is predominantly determined by the lowest MC tree in the small c limit. If s is a positive integer, the lowest MC tree for an $N(=2^s)$ -spin chain is constructed by excluding all the branches beginning with a mode having more than $s + 1$ spins in the MC tree for the N -spin chain. The number of spins in each mode is less than or equal to $(s + 1)$ for the lowest MC tree, and the leading term of $\tau_1(N)$ is given by $\tau_1(N) \xrightarrow{c \rightarrow 0} \mathcal{O}(c^{-s-1})$, which is also valid for an N -spin ($2^s \leq N < 2^{s+1}$) chain. The lowest MC tree for an eight-spin chain is shown in Figure 4 as another example. The proofs for an arbitrary chain of finite length are given in refs 11–16.

The mean relaxation time τ_1 for an infinite spin chain is derived from $\lim_{N \rightarrow \infty} \tau_1(N)$. Simulations and theoretical calculations have shown that the relaxation of spin 0 is mainly controlled by the first up-spin on the right.^{7,12–15} Because the mean distance between two adjacent up-spins is c^{-1} in equilibrium, it is reasonable to set $N = c^{-1}$ as the effective chain length of the infinite spin chain, giving $\tau_1 \xrightarrow{c \rightarrow 0} \mathcal{O}(c^{\log_2 c})$. This result has been derived rigorously elsewhere.^{11–16}

B. Slow Dynamics of Nonlinear Modes. In the previous subsection, we discussed the dynamic scaling of the East model by studying τ_1 . As the products of linear modes, the relaxation of nonlinear modes also becomes slow as $c \rightarrow 0$. By studying

$C_k^r(t)$ and $C_k(t)$, we investigate slow dynamics of nonlinear modes in this subsection. In the small c limit, τ_1 scales as $\tau_1 \sim \mathcal{O}(c^{-s})$, where $s \sim \mathcal{O}(\log_2 c^{-1}) \xrightarrow{c \rightarrow 0} \infty$. The mean relaxation time for the second-order reduced correlation function is

$$\tau_2^r = \hat{C}_2^r(0) = \frac{c - \tau_1^{-1}}{c(1 - c)} \approx 1 + c + \mathcal{O}(c^2) \quad (18)$$

where τ_2^r differs from τ_1 in the order of c and does not diverge in the small c limit. By definition, we have

$$\begin{aligned} \tau_1 &= -(\mathbf{L}^{-1})_{1,1} = -\langle f_{\text{eq}} q_1 \mathbf{L}^{-1} q_1 \rangle \\ \tau_2^r &= -[(\mathbf{L}_2^r)^{-1}]_{1,1} = -\langle f_{\text{eq}} q_2 (\mathbf{L} \mathbf{Q}_1)^{-1} q_2 \rangle \end{aligned} \quad (19)$$

where projection operators are defined as $\mathbf{P}_k = q_k \langle f_{\text{eq}} q_k \rangle$ and $\mathbf{Q}_k = \mathbf{I} - \sum_{m=1}^k \mathbf{P}_m$. Here we emphasize the notations of the *complete dynamic space* and the *projected dynamic space*, which are frequently used in this article. The complete dynamic space Γ_0 includes all modes influencing the relaxation of spin 0, i.e., all modes with the same first spin 0. A projected dynamic space is a subspace of the Γ_0 by projecting out one or more relevant modes, e.g., $\mathbf{Q}_1 \Gamma_0 = \Gamma_0 - \{A_1(0)\}$. As a result, τ_1 is calculated over the complete space Γ_0 , whereas τ_2^r is calculated over the projected space $\mathbf{Q}_1 \Gamma_0$. Next we calculate the mean relaxation time of the second-order full correlation function over Γ_0 ,

$$\tau_2 = \hat{C}_2(0) = -(\mathbf{L}^{-1})_{2,2} = -\langle f_{\text{eq}} q_2 \mathbf{L}^{-1} q_2 \rangle \approx \mathcal{O}(c^{-s+1}) \approx c \tau_1 \quad (20)$$

The slow dynamics of q_2 is described by $C_2(t)$ over Γ_0 instead of $C_2^r(t)$ over $\mathbf{Q}_1 \Gamma_0$. Another interesting result is that the simple Gaussian factorization scheme is not valid in the East model because of asymmetrical kinetic constraints.⁸ For $q_2 = \{A_2(01)\}$, the kinetics of spin 0 is controlled by the state of spin 1, whereas spin 1 is independent of spin 0. From this microscopic picture, a reasonable factorization scheme is $C_2(t) \approx c C_1(t)$ where spin 0 achieves equilibrium quickly and spin 1 has a slow relaxation. Equation 20 is consistent with this factorization scheme. We

extend the calculation of the mean relaxation times to the third order, obtaining

$$\begin{aligned}\tau_3^r &= -[(L_3^r)^{-1}]_{1,1} \approx 1 + c + \mathcal{O}(c^2) \\ \tau_3 &= -(L^{-1})_{3,3} \approx \mathcal{O}(c^{-s+2}) \approx c^2 \tau_1 \approx c \tau_2\end{aligned}\quad (21)$$

The slow dynamics of q_3 is again described by $C_3(t)$ over Γ_0 whereas $C_3^r(t)$ over a projected space $\mathbf{Q}_2\Gamma_0$ is fast.

Although the above argument is specifically derived for the East model, a preference of full correlation functions to reduced correlation functions for slow dynamics of nonlinear modes is universal in dissipative systems. To demonstrate this preference, we invert an arbitrary kinetic matrix L to calculate $\tau_k^r = -[(L_k^r)^{-1}]_{1,1}$ and $\tau_k = -(L^{-1})_{k,k}$. We demonstrate in the first subsection of Appendix B that the mean relaxation times of the full and reduced correlation functions are related as

$$\tau_k^{-1} = (\tau_k^r)^{-1} - \Omega_k^L \quad (22)$$

where $\Omega_k^L \equiv \Omega_k^L(z=0)$ is defined in eq B6 and includes kinetic contributions from basis sets lower than q_k . Because of kinetic constraints ($\Omega_k > 0$), $0 < \tau_k^r < \tau_k$ holds for $k \geq 2$. Near the divergence point of the East model, $\tau_k \rightarrow \infty$ and $0 < \tau_k^r \sim \Omega_k^L \ll \tau_k$ are valid, indicating that $C_k(t)$ always decays much slower than $C_k^r(t)$ in the long time. In summary, full correlation functions $C_k(t)$ defined in the complete dynamic space describe slow dynamics of nonlinear modes, whereas memory kernels $M_k(t)$ and the corresponding reduced correlation functions $C_k^r(t)$ defined in projected dynamic spaces are not necessarily slow.

C. Irreducible Memory Kernel. In this subsection, we extend slow dynamics of nonlinear modes to explore the nature of the irreducible memory kernel. Explicit expressions of $\hat{C}_2^{\text{ir}}(z)$ and $\hat{C}_2(z)$ are

$$\begin{aligned}\hat{C}_2^{\text{ir}}(z) &= [z\mathbb{I} + \Omega_2 - \Omega_2^L - \hat{M}_2(z)]^{-1} \\ &= [z\mathbb{I} + \Omega_2 - L_{2,1}\Omega_1^{-1}L_{1,2} - \hat{M}_2(z)]^{-1}\end{aligned}\quad (23)$$

$$\begin{aligned}\hat{C}_2(z) &= [z\mathbb{I} + \Omega_2 - \Omega_2^L(z) - \hat{M}_2(z)]^{-1} \\ &= [z\mathbb{I} + \Omega_2 - L_{2,1}(z\mathbb{I} + \Omega_1)^{-1}L_{1,2} - \hat{M}_2(z)]^{-1}\end{aligned}\quad (24)$$

where $\hat{C}_2^{\text{ir}}(z)$ is the second-order *irreducible correlation function*, which is related to the irreducible memory kernel by $\hat{M}_1^{\text{ir}}(z) = L_{1,2}\hat{C}_2^{\text{ir}}(z)L_{2,1}$. To be consistent with our previous discussions of $C_k^r(t)$ and $C_k(t)$, we analyze $C_2^{\text{ir}}(t)$ instead of $M_1^{\text{ir}}(t)$. In Appendix C, we present a detailed proof of the equivalence between the matrix expression of $C_2^{\text{ir}}(t)$ in eq 23 and the operator expression of $M_1^{\text{ir}}(t)$ introduced by Kawasaki.¹⁸ From eqs 23 and 24, the difference between $\hat{C}_2^{\text{ir}}(z)$ and $\hat{C}_2(z)$ is a term involving q_1 , which behaves as Ω_1^{-1} in $\hat{C}_2^{\text{ir}}(z)$ and as $(z\mathbb{I} + \Omega_1)^{-1}$ in $\hat{C}_2(z)$. As a result, these two correlation functions have different initial behaviors, $C_2^{\text{ir}}(t) \approx \exp[-(\Omega_2 - \Omega_2^L)t]$, $C_2(t) \approx C_2^r(t) \approx \exp(-\Omega_2 t)$, and $C_2^{\text{ir}}(t) > C_2(t)$ for $t \rightarrow 0$, but both have slow relaxations with the same mean relaxation time, $\hat{C}_2^{\text{ir}}(0) = \hat{C}_2(0)$.

As shown in the second subsection of Appendix C, we construct the k th-order irreducible correlation function,

$$\hat{C}_k^{\text{ir}}(z) = [z\mathbb{I} + \Omega_k - \Omega_k^L - \hat{M}_k(z)]^{-1} \quad (25)$$

where z dependence in $\Omega_k^L(z)$ is omitted, $\Omega_k^L = \Omega_k^L(z=0)$. To be complete, a recursive expression for $\hat{C}_k^{\text{ir}}(z)$ is derived in eq B12. In comparison to $C_k(t)$, $C_k^{\text{ir}}(t)$ has slower initial but similar long-time behavior. Although there are other choices for nonlinear slow functions based on modifying either $\hat{C}_k(z)$ or $C_k(t)$, we restrict analysis to $C_k(t)$ and $C_k^{\text{ir}}(t)$ in this article.

In summary, we observe that full and irreducible correlation functions are slow functions, whereas reduced correlation functions and memory kernels are relatively fast in dissipative systems. The microscopic cause of the difference is that low-order modes are slow. Relaxations of nonlinear modes in the long time are strongly affected by the interaction with slow modes. Once lower order modes are projected out, the resulting reduced correlation functions and memory kernels fail to capture the slow relaxation of nonlinear modes. The recursive expressions for $C_k(t)$ and $C_k^{\text{ir}}(t)$ appear in Appendix B and are applicable in other dissipative systems, e.g., colloids.²²

V. Simple Mode Coupling(SMC)

In the remainder of this article, we discuss the relationships of $C_k^{\text{ir}}(t)$ and $C_k(t)$ with MC closures and other nonperturbative approximations. Studying such a simple kinetic system can help us improve our understanding of MC in the regime of $T_g \leq T \leq T_c$. The first-order simple mode coupling(SMC) approximation is derived in this section after comparing $C_2^{\text{ir}}(t)$ with $C_1(t)$. The second-order SMC based on $C_2(t)$ and $C_3^{\text{ir}}(t)$ is found to improve the accuracy of predictions of $C_1(t)$ but introduces the same unphysical phenomena of the ergodic to nonergodic transition at small c as the first-order SMC.

A. First-Order SMC. The second-order irreducible correlation function is obtained from eq 23,

$$\begin{aligned}\hat{C}_2^{\text{ir}}(z) &= \left[z + 1 - \frac{c(1-c)}{c} - \hat{M}_2(z) \right]^{-1} \\ &= [z + c - \hat{M}_2(z)]^{-1}\end{aligned}\quad (26)$$

Comparing eq 26 with $\hat{C}_1(z) = [z + c - \hat{M}_1(z)]^{-1}$, we find that $C_2^{\text{ir}}(t)$ has the same initial decay as $C_1(t)$, $\lim_{t \rightarrow 0} C_2^{\text{ir}}(t) \approx C_1(t) \sim e^{-ct}$, which makes $C_2^{\text{ir}}(t)$ a better choice than $C_2(t)$ in the first-order SMC. Analysis of τ_1 and τ_2 gives a long-time expression, $\hat{C}_2^{\text{ir}}(0) \approx \hat{C}_1(0) \sim \mathcal{O}(c^{-s})$, where the slight difference between the orders of c is ignored because $s \sim \mathcal{O}(\log_2 c^{-1}) \xrightarrow{c \rightarrow 0} \infty$. Similarities between $C_2^{\text{ir}}(t)$ and $C_1(t)$ at both short and long times suggest a reasonable linear MC closure,

$$C_2^{\text{ir}}(t) \approx C_1(t) \quad (27)$$

which is the SMC approximation proposed by Pitts and Andersen using a diagrammatic method.^{19,20} The equivalence between the diagrammatic method and the complete basis set formalism is demonstrated in Figure 5. Note that eq 27 is not consistent with our factorization argument in section IVB, $\lim_{t \rightarrow \infty} C_2(t) \approx cC_1(t)$, which will be explored to improve SMC in section VIB. Substituting eq 27 into

$$\hat{C}_1(z) = \{z + c[1 + (1-c)\hat{C}_2^{\text{ir}}(z)]^{-1}\}^{-1} \quad (28)$$

gives a self-consistent SMC equation,

$$\hat{C}_1^{\text{SMC}}(z) = \left[z + \frac{c}{1 + (1-c)\hat{C}_1^{\text{SMC}}(z)} \right]^{-1} \quad (29)$$

which was first proposed by Pitts and Andersen.^{19,20}

	Pitts and Andersen's diagrammatic expressions	Matrix expressions
L		$L_{m,m} ; L_{m,m \pm 1}$
$M_1(z)$		$L_{1,2} C_2^s(z) L_{2,1}$
$M_1^r(z)$		$L_{1,2} C_2^r(z) L_{2,1}$
SMC		$C_2^r(z) = C_1(z)$
EMC $\Delta(z)$		$C_2^r(z) = \frac{C_1(z)}{1 + \Delta(z) C_1(z)}$

Figure 5. One-to-one correspondence between Pitts and Andersen's diagrammatic method and the matrix formalism.

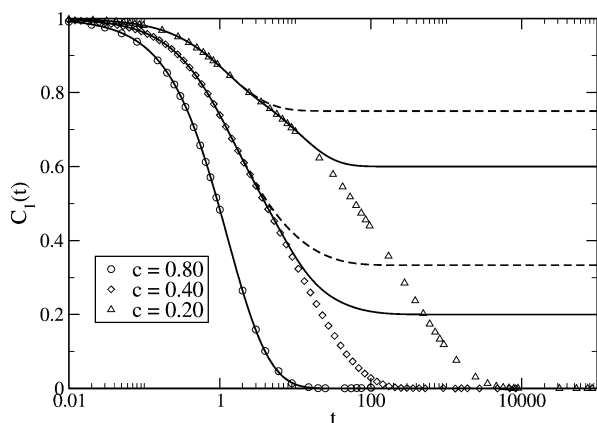


Figure 6. Comparison of $C_1(t)$ from the first- and second-order SMC approximations and from simulations for $c = 0.2, 0.4, \text{ and } 0.8$. The dashed lines are the first-order SMC results calculated from eq 29. The solid lines are the second-order SMC results calculated from eq 35. The symbols are simulation results.

In Figure 6, we plot $C_1^{\text{SMC}}(t)$ for $c = 0.8, 0.4, \text{ and } 0.2$. Predictions of $C_1^{\text{SMC}}(t)$ are accurate in the short time because of $\lim_{t \rightarrow 0} C_2^{\text{ir}}(t) \sim C_1(t)$, and for large values of c ,²⁰ but $C_1^{\text{SMC}}(t)$ becomes much less reliable as c or T decreases and predicts an unphysical plateau for $c \leq 0.5$, $\lim_{t \rightarrow \infty} C_1^{\text{SMC}}(t) = (1 - 2c)/(1 - c) \geq 0$. The appearance of this plateau corresponds to a SMC transition point at $c_c = 0.5$ ($T_c = \infty$), which is different from the real divergence point, $c_g = 0$ ($T_g = 0$). Figure 7 shows that each mode in the MC tree for $\hat{C}_2^{\text{ir}}(z)$ is replaced by lower order

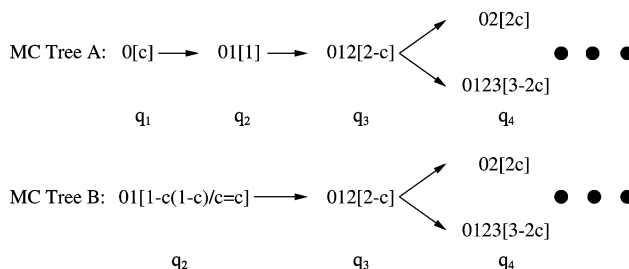


Figure 7. Two MC trees for the first-order SMC approximation. As an abbreviation of Figure 1, MC tree A corresponds to $\hat{C}_1(z)$, whereas MC tree B is for $\hat{C}_2^{\text{ir}}(z)$, where the eigenfrequency of mode $A_2(01)$ is modified to $(\Omega_2 - \Omega_2^L)$.

modes, e.g., $A_3(012)$ is replaced by $A_2(01)$, so that $\hat{C}_2^{\text{ir}}(z)$ is overestimated and we have $T_c > T_g$. One can further understand the first-order SMC through a continued fraction,

$$\hat{C}_1^{\text{SMC}}(z) = 1/z + c - c(1 - c)/z + 1 - c(1 - c)/z + 1 - \dots \quad (30)$$

which corresponds to a MC tree without branches,

$$0[c] \rightarrow 01[1] \rightarrow 12[1] \rightarrow 23[1] \rightarrow \dots \rightarrow (i, i + 1)[1] \rightarrow \dots \quad (31)$$

indicating that the first-order SMC is a mean-field approximation in which each spin is affected by a two-spin segment. Only two eigenfrequencies, $\Omega_1 = c$ and $\Omega_2 = 1$, appear in the partial resummation. However, simulations and theoretical calculations suggest that $C_1(t)$ is a weighted average over domains at low T .¹⁵

Our calculations of the East model suggest serious deficiencies of MC in the temperature regime between T_g and T_c . For dissipative and nondissipative liquids, we find that a four-point correlation function is similarly overestimated by the Gaussian factorization scheme.^{22,28} Recently, Schweizer combined the MC approximation with a hopping model by a phenomenological potential and significantly improved the prediction of the glass transition point in a hard-sphere liquid.^{29,30} However, it remains a challenge to develop a microscopic technique to predict a crossover from the MC trapping to the hopping process for $T_g < T < T_c$.

B. Second-Order SMC. We now extend Andersen's SMC to higher orders. Although different MC closures are possible, a simple calculation involving $C_3^{\text{ir}}(t)$ and $C_2(t)$ is presented as an example of higher order SMC approximations. Explicit expressions of $\hat{C}_2(z)$ and $\hat{C}_3^{\text{ir}}(z)$ are

$$\hat{C}_2(z) = \left[z + 1 - \frac{c(1-c)}{z+c} - \hat{M}_2(z) \right]^{-1} \quad (32)$$

$$\begin{aligned} \hat{C}_3^{\text{ir}}(z) &= \left[z + 2 - c - \frac{c(1-c)}{1 - \frac{c(1-c)}{c}} - \hat{M}_3(z) \right]^{-1} \\ &= [z + 1 - \hat{M}_3(z)]^{-1} \end{aligned} \quad (33)$$

respectively. The initial relaxations of these two functions are the same, $\lim_{t \rightarrow 0} C_2(t) \approx C_3^{\text{ir}}(t) \sim e^{-t}$. The integrated lifetimes, τ_2 and τ_3 , give a long-time relationship, $\hat{C}_2(0) \approx \hat{C}_3^{\text{ir}}(0) \sim O(c^{-s})$, where we once again ignore the slight difference in the orders of c . Because of these two limiting relationships, a linear SMC closure,

$$C_3^{\text{ir}}(t) \approx C_2(t) \quad (34)$$

gives

$$\hat{C}_2^{\text{SMC}}(z) = \left[z + 1 - \frac{c(1-c)}{z+c} - \frac{c(1-c)\hat{C}_2^{\text{SMC}}(z)}{1 + (1-c)\hat{C}_2^{\text{SMC}}(z)} \right]^{-1} \quad (35)$$

which is used to obtain $C_1(t)$.

In Figure 6, we compare $C_1(t)$ predicted from eqs 29 and 35 and simulations for $c = 0.8, 0.4$, and 0.2 . Although a rigorous calculation shows that the transition point predicted by eq 35 is the same as that by eq 29, $c_c = 0.5$ ($T_c = \infty$), the value of the long-time plateau of $C_1(t)$ decreases from $(1-2c)(1-c)^{-1}$ to $(1-2c)$ for $c \leq 0.5$. Rewriting eq 35 as a continued fraction,

$$\hat{C}_2^{\text{SMC}}(z) = 1/z + 1 - \frac{c(1-c)}{z+c} - c(1-c)/z + 2 - c - \frac{c(1-c)}{z+c} - c(1-c)/\dots \quad (36)$$

reveals that the second-order SMC is a mean-field approximation in which three-spin segments are involved. Similar results can be found for other higher order SMC approximations. Recently, Szamel improved the MC prediction of the glass transition point in the hard-sphere Brownian liquid by the second-order calculation.³¹ Our results for the East model suggest that higher order MC approximations have the potential to predict the glass transition but difficulties remain.²²

In this section, we derived two SMC approximations for the East model, through comparisons between $C_1(t)$ and $C_2^{\text{ir}}(t)$, and

between $C_2(t)$ and $C_3^{\text{ir}}(t)$, respectively. Our calculations suggest that SMC has difficulties for $T_g \leq T \leq T_c$ because the partial resummation overestimates slow functions of nonlinear modes, e.g., $C_2^{\text{ir}}(t)$. The second-order SMC improves prediction but still fails to remove the unphysical plateau.

VI. Nonlinear Closures beyond SMC

Discussions in the previous section show deficiencies of SMC approximations in the regime between T_g and T_c . In this section, we study two alternative MC methods and in next section, we study a numerical approach on the basis of domain dynamics.

A. Extended Mode Coupling (EMC). As c decreases, detailed nonlinear kinetics in the East model become increasingly important and cannot be simplified as in SMC. Exact expressions for $\hat{C}_1(z)$ and $\hat{C}_2^{\text{ir}}(z)$ suggest

$$\begin{aligned} \hat{C}_2^{\text{ir}}(z) &= \{z + c - \hat{M}_1(z) + [\hat{M}_1(z) - \hat{M}_2(z)]\}^{-1} \\ &= [\hat{C}_1^{-1}(z) + \Delta(z)]^{-1} \end{aligned} \quad (37)$$

where a difference function is defined as $\Delta(z) \equiv \hat{M}_1(z) - \hat{M}_2(z)$. Substituting eq 37 into eq 28 gives the self-consistent equation,

$$\hat{C}_1^{\text{EMC}}(z) = \left\{ z + c - \frac{c(1-c)}{[\hat{C}_1^{\text{EMC}}(z)]^{-1} + \Delta(z) + 1 - c} \right\}^{-1} \quad (38)$$

which is consistent with Andersen's extended mode coupling (EMC) approximation. In ref 20, Pitts and Andersen obtained expressions for $\Delta(z)$ through a set of diagrams, which represents corrections to SMC. Here eq 37 gives an explicit definition of $\Delta(z)$ that allows systematic calculations. Figure 5 demonstrates the relationship between the matrix and diagrammatic approaches.

We evaluate $\Delta(z)$ by basis set expansion. To be consistent with section III, the order of $\Delta(z)$ is defined by the order of the highest basis set involved in the calculation. For example, truncated at q_2 , we get $\Delta^{(2)}(z) = c(1-c)(z+1)^{-1}$; $\Delta^{(3)}(z)$ is truncated at q_3 ,

$$\Delta^{(3)}(z) = \frac{c(1-c)}{z + 1 - \frac{c(1-c)}{z + 2 - c}} - \frac{c(1-c)}{z + 2 - c} \quad (39)$$

In Figure 8, we plot $C_1^{\text{EMC}}(t)$ evaluated by $\Delta^{(3)}(z)$ and $\Delta^{(6)}(z)$ along with simulations for $c = 0.4$ and 0.2 . The persisting long-time plateau of $C_1^{\text{SMC}}(t)$ is removed. Comparing Figures 2 and 8, $C_1^{\text{EMC}}(t)$ and $C_1^{(k)}(t)$ at the same order are indistinguishable. To understand these results, we rewrite eq 38 as

$$\begin{aligned} \hat{C}_1^{\text{EMC}}(z) &= \\ &1/z + c - c(1-c)/z + 1 + \Delta(z) - c(1-c)/\dots \end{aligned} \quad (40)$$

Because $\Delta(0) \sim O(c^{s-1}) > 0$, we have $C_1^{\text{EMC}}(t) \xrightarrow{t \rightarrow \infty} 0$ and the plateau is removed. Expanding $\Delta^{(k)}(z)$ in eq 37, the leading term of $\hat{C}_1^{\text{EMC}}(z)$ is

$$\begin{aligned} \hat{C}_1^{\text{EMC}}(z) &\approx \\ &1/z + c - c(1-c)/z + 1 - c(1-c)/\dots/z + \Omega_k \end{aligned} \quad (41)$$

which is indistinguishable from $C_1^{(k)}(t)$ at the same order. Equation 41 also shows that the reliable prediction of $C_1^{\text{EMC}}(t)$ at a given c is obtained through expansion to order of c^{-1} ,

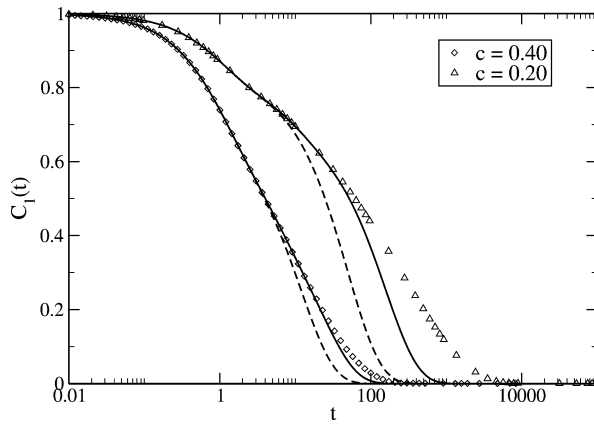


Figure 8. Comparison of $C_1(t)$ from the EMC approximations and from simulations for $c = 0.2$ and 0.4 . Using eq 39, the dashed lines are calculated from $\Delta^{(3)}(z)$ truncated at q_3 . Similarly, the solid lines are calculated from $\Delta^{(6)}(z)$ truncated at q_6 and cannot be distinguished from $C_1^{(6)}(t)$ by basis set expansion in Figure 2. The symbols are simulation results.

indicating that the EMC approximation is not practical in the small c limit if $\Delta(z)$ is evaluated perturbatively.

B. Long-Time Correction. We introduce a long-time correction by considering accurate asymptotic relationships. In the first-order SMC, the short-time similarity between $C_1(t)$ and $C_2^{ir}(t)$ is guaranteed, but the different long-time c dependence is ignored. Assuming two limiting expressions $\hat{M}_1(0) \approx c - \mathcal{O}(c^s)$ and $\hat{M}_2(0) \approx c - \mathcal{O}(c^{s-1})$ can be extended to the whole z axis, we have

$$\hat{M}_1(z) \approx c + c[\hat{M}_2(z) - c] \quad (42)$$

Using eq 42 as a closure, we have a new self-consistent equation,

$$\hat{C}_1^{LT(2)}(z) = \left\{ z + c - \frac{c^2(1-c)}{[\hat{C}_1^{LT(2)}(z)]^{-1} - (1-c)(z-c)} \right\}^{-1} \quad (43)$$

where the superscript 2 in $\hat{C}_1^{LT(2)}(z)$ indicates that the long-time correction is applied to the second-order memory kernel. Although this correction removes the plateau in $C_1^{SMC}(t)$, the underestimation of $\hat{M}_1(t)$ in the short time makes $\hat{C}_1^{LT(2)}(t)$ decay much faster than simulations in the long time. A long-time correction based on $\hat{M}_2(z)$ and $\hat{M}_3(z)$ gives

$$\hat{C}_1^{LT(3)}(z) = \left\{ z + c - \frac{c(1-c)}{z + 1 - \frac{c^3(1-c)}{[\hat{C}_1^{LT(3)}(z)]^{-1} + c^2(1-c) - (1-c^2)z}} \right\}^{-1} \quad (44)$$

Calculating $\hat{M}_3(z)$ and $\hat{M}_4(z)$ in the eight-spin chain, we obtain another long-time correction,

$$\hat{M}_3(z) \approx \frac{c^2(1-3c^2-c^3-c^5)[\hat{C}_1^{LT(4)}(z)]^{-1} - (1-c)(1+c)[z-c^2(1+c)^2]}{(1-c)\{[\hat{C}_1^{LT(4)}(z)]^{-1} + c^2(1+c)^2 - z\}^2} \quad (45)$$

which is solved self-consistently with $\hat{C}_1^{LT(4)}(z)$. In Figure 9, we compare $C_1^{LT}(t)$ predicted by these three long-time corrections and from the simulation for $c = 0.2$. We find that $C_1^{LT(4)}(t)$

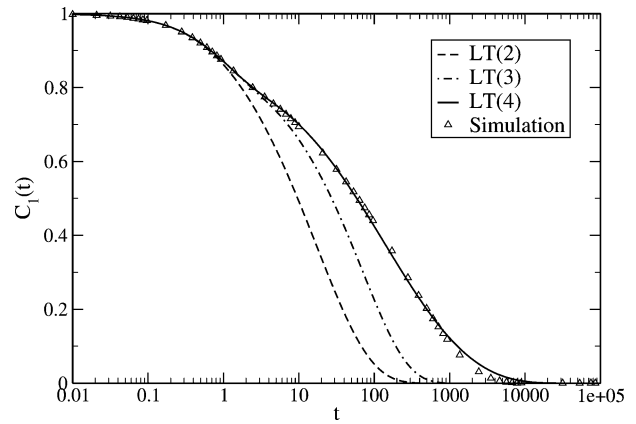


Figure 9. Comparison of $C_1(t)$ from long-time corrections and from simulations for $c = 0.2$. The dashed line is the long-time correction result calculated from eq 43. The dot-dashed line is calculated from eq 44. The solid line is calculated from substituting eq 45 into eq 13. The symbols are the simulation results.

agrees with the simulation in a broad temporal range, but one must still truncate the expansion at high orders for small values of c .

In this section, we developed two MC-based methods to improve SMC. Although the incorrect long-time plateau of $C_1^{SMC}(t)$ is removed by both methods, the improvement of predictive power depends on the truncation of the basis set, scaling as c^{-1} for $c \rightarrow 0$. EMC results are indistinguishable from those by the basis set expansion, whereas the long-time correction method becomes less systematic as truncation order increases. In general, MC-based closures become difficult near the glass transition point because of cooperative motions on large scales.

VII. Stretched Exponential Form

From the previous sections, we find that the analytic methods associated with the basis set expansion are not practical in the small c limit. In this section, we discuss the stretched exponential form, which is commonly applied to systems exhibiting slow dynamics. In principle, the correlation function $C_A(t)$ for a many-particle system can be obtained by averaging over all the configurations,

$$C_A(t) = \sum_L \rho(L) C_A(L, t) \quad (46)$$

where $\rho(L)$ is the equilibrium density of a configuration L , and $C_A(L, t)$ is the correlation function associated with this configuration. Although kinetics differ as L varies, a scaling behavior is valid in many systems,³² $C_A(L, t) \approx G[t/\tau(L), \{\alpha_L\}]$, where G is a scaling function, $\tau(L)$ is the relaxation time associated with configuration L , and $\{\alpha_L\}$ is a relevant parameter set dependent on L . This scaling has been demonstrated for the large length and long-time scales.^{14,33}

Our scaling argument for the East model is motivated by Garrahan and Chandler's study of domain dynamics.⁹ As we mentioned in section IVA, simulations and theoretical calculations indicate that the relaxation of spin 0 is mainly controlled by the first up-spin on the right. Down spins between two adjacent up-spins form a dynamic domain L , the size of which is denoted by l . Because kinetic contributions from spins outside L are negligible before L relaxes, the relaxation of spin 0 is approximated as a weighted average over all the domains ($0 \leq l < \infty$). In the continuum limit, the equilibrium domain density

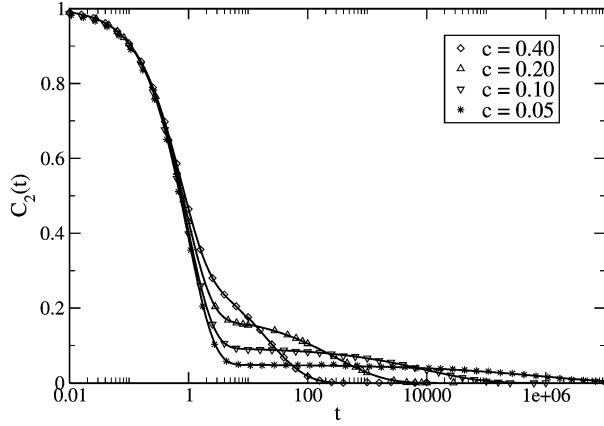


Figure 10. Comparison of $C_2(t)$ from simulations and the stretched exponential approximation for $c = 0.4, 0.2, 0.1,$ and 0.05 . The symbols are simulation results. The solid lines are calculated from eq 49, where b , τ , and β are fitting parameters as shown in Table 1.

is given by a Poisson distribution, $\rho_{\text{eq}}(l) = ce^{-cl}$, which gives

$$C_1(t) \approx \int_0^\infty dl ce^{-cl} C_1(l, t) \quad (47)$$

where $C_1(l, t)$ is the correlation function for a domain of size l . In the second article on the East model from our group,³⁴ $C_1(l, t)$ is evaluated by simulating domain lifetimes; the corresponding averaged lifetime accurately reproduces $C_1(t)$ except for short times. The initial relaxation is mainly controlled by a first few modes, which differs from domain dynamics. For simplicity, we evaluate $C_1(l, t)$ with a simple exponential form, $C_1(l, t) \approx \exp\{-t/\tau(l)\}$, where $\tau(l)$ is the mean relaxation time for a finite chain, $\tau(l) \sim \mathcal{O}(c^{-\log_2 l})$. Using the saddle point approximation, $(\partial/\partial l) \exp\{-[cl + c^{\log_2 l} t]\}_{l_m} = 0$, a crude estimate of $C_1(t)$ in eq 47 is

$$C_1(t) \approx \int_0^\infty dl ce^{-cl} \exp(-tc^{\log_2 l}) \\ \sim e^{-cl_m(t)} \exp\{-t[l_m(t)]^{\log_2 c}\} \sim e^{-ct^\beta} \quad (48)$$

where $\lim_{c \rightarrow 0} \beta \sim \mathcal{O}([\log_2 c^{-1}]^{-1}) \rightarrow 0$ is applied. Thus, the long-time decay of $C_1(t)$ follows a stretched exponential, which was first shown by Garrahan and Chandler.⁹

The stretched exponential is applicable in the long-time limit and cannot describe $C_1(t)$ in a broad temporal range. In fact, the simulation by Andersen and co-workers indicates the lack of evidence for exponential or stretched exponential behavior over a broad range of time scales.¹⁹ Recently, Sollich and Evans argued that a real functional form of $C_1(t)$ is more complicated than eq 48.^{14,15} The fact that predictions of $C_1(t)$ are improved by high-order SMC suggests testing the stretched exponential form for slow functions of nonlinear modes. To facilitate comparisons with simulations, we consider $C_2(t)$ instead of $C_2^{\text{ir}}(t)$. Simulations in Figure 10 suggest that $C_2(t)$ exhibits a clear time-scale separation. A multiexponential function from the basis set expansion truncated at q_5 is applied in the short time, whereas a stretched exponential is fitted in the long time. The overall fitting function is

$$C_2(t) \approx C_2^{(5)}(t)\Theta(t_0 - t) + C_2^{\text{fit}}(t)\Theta(t - t_0) \\ = \sum_{i=1}^8 a_i e^{-\omega_i t} \Theta(t_0 - t) + b e^{-(t/\tau)^\beta} \Theta(t - t_0) \quad (49)$$

where the perturbation function $C_2^{(5)}(t)$ with $\{a_i\}$ and $\{\omega_i\}$ is

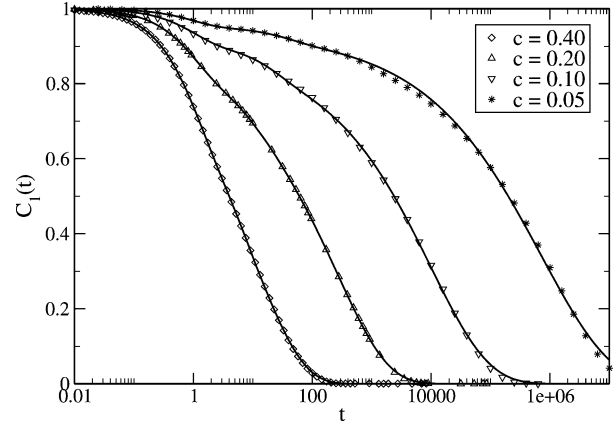


Figure 11. Comparison of $C_1(t)$ from simulations and from the asymptotic approximation for $c = 0.4, 0.2, 0.1,$ and 0.05 . The solid lines are calculated by substituting $C_2(t)$ from eq 49 into eq B8. The symbols are simulation results.

TABLE 1: Fitting Parameters for $C_2^{\text{fit}}(t)$ in Eq 49

c	b	τ	β	t_0
0.40	0.3358	1.937×10	0.6483	4.174
0.20	0.1839	2.989×10^2	0.5339	5.290
0.10	0.09474	9.732×10^3	0.4443	36.93
0.05	0.04911	8.122×10^5	0.3346	149.1

truncated at q_5 similar to $C_1^{(5)}(t)$, and an asymptotic function $C_2^{\text{fit}}(t)$ is fitted by three parameters, b , τ , and β . Here, $\Theta(t)$ is the Heaviside step function, and t_0 is determined by $C_2^{(5)}(t_0) = C_2^{\text{fit}}(t_0)$. The fast equilibration of spin 0 in $A_2(01)$ determines $b \sim \mathcal{O}(c)$, and $\tau \sim \mathcal{O}(c^{\log_2 c})$ and $\beta \sim \mathcal{O}([\log_2 c^{-1}]^{-1})$ are determined by eq 48. As shown in Figure 10, $C_2^{\text{fit}}(t)$ agrees with simulations for several values of c . Equation 49 is valid not only for small values of c (0.05) but also for intermediate values (0.4). The stretched exponential form is applicable to $C_2(t)$ over a wide temperature range. Next we calculate $C_1(t)$ from $C_2(t)$ by substituting eq 49 into eq B8. The results are plotted with simulations in Figure 11, exhibiting agreement in the whole temporal range. The fitting parameters for each value of c are displayed in Table 1. As a convolution of $C_2^{\text{fit}}(t)$, $C_1(t)$ has a more complicated form than the stretched exponential.

In summary, we discussed the stretched exponential form arising from domain dynamics. The second-order correlation function $C_2(t)$ is fitted phenomenologically to a stretched exponential in the long time, and calculated according to truncated basis set expansion in the short time. Using the matched $C_2(t)$, we find agreement between the approximated $C_1(t)$ and simulations. Compared to analytical methods in the previous sections, this functional form describes kinetics near the glass transition point. However, as a first-principle theory, we need to develop more systematic approaches to describe domain dynamics.

VIII. Conclusions and Discussions

A. Summary of Results. In this article we systematically analyze kinetics of the East model on the basis of the complete basis set and the kinetic matrix L . A mode coupling (MC) tree is designed to organize the infinite matrix L . The finite-order truncation of the complete basis set leads to a systematic approach to calculate the single-spin self-correlation function. The complete basis set is general and can be applied to other dissipative systems. For example, in our recent article on a 2D rotor lattice, we calculated reorientational relaxation in the

intermediate temperature range using the same method.²¹ Applications to colloids have produced promising results in predicting glass transition points.²² Our matrix calculation in the complete basis set not only recovers earlier results obtained through the projection operator technique but also provides new insights into the irreducible memory kernels, mode coupling and ergodic to nonergodic transitions. Our effort establishes a one-to-one correspondence between the elegant diagram theory by Pitts and Andersen²⁰ and our matrix formalism, as shown in Figure 5.

An important observation of this article is a characteristic feature of dissipative systems: *full and irreducible correlation functions defined in the complete dynamic space are categorized as slow functions, whereas reduced correlation functions and memory kernels defined in projected spaces are relatively fast and do not capture the slow relaxation of nonlinear modes.* On the basis of this observation, we clarify the nature of the irreducible memory kernel introduced by Cichocki and Hess,²³ Kawasaki,¹⁸ and Pitts and Andersen.²⁴ For the East model and dissipative systems in general, we can systematically derive recursive expressions for slow or fast functions, which is the starting point of applying MC closures and asymptotic relations.

Applying the algebraic relations between $C_1(t)$ and $C_2^{\text{ir}}(t)$ in the East model, we find $C_2^{\text{ir}}(t) \approx C_1(t)$ at short time and $\int_0^\infty C_2^{\text{ir}}(t) dt \approx \int_0^\infty C_1(t) dt$ at low temperatures, which leads to the SMC closure, $C_2^{\text{ir}}(t) \approx C_1(t)$, first proposed by Andersen and co-workers.^{19,20} Although the first-order SMC approximation provides reliable predictions of $C_1(t)$ for large c , it fails for $c \leq 0.5$, predicting the transition point at $c_c = 0.5$ instead of $c_g = 0$. As a mean-field approximation, the first-order SMC cannot describe cooperative motions on large length scales. In comparison, the second-order SMC improves the agreement but fails to remove the emerging plateau at T_c , indicating the difficulty of describing the slow but finite relaxation in the East model using a mean-field approach.

Two analytic methods, EMC and long-time correction, extend SMC. By introducing a difference function into the irreducible memory kernel to account for nonlinear kinetics, we recovered Andersen's EMC approximation.²⁰ The long-time correlation method is obtained from new MC closures based on asymptotic relationships. These analytic methods predict the correct divergence point, $c_g = 0$, and can reliably predict $C_1(t)$ by increasing the order of approximation. However, the minimum truncation order to reliably predict $C_1(t)$ from these two methods scales as c^{-1} , indicating the difficulties of these methods in the small c limit.

Hierarchical domain dynamics in the East model have been explored recently.^{9,10,12-15} Using the saddle point argument, we obtained a stretched exponential form. The second-order full correlation function $C_2(t)$ is found to have time-scale separation and becomes a natural candidate for the basis set expansion in the short time and the stretched exponential approximation in the long time. The resulting $C_1(t)$ agrees with simulations and supports indirectly the notion of domain dynamics in the long time at low temperatures.

The East model is probably one of the simplest nontrivial dissipative systems that exhibit dynamic slow-down and divergence of time scales at low temperatures. The simplicity of the East model provides a unique opportunity to construct the mode coupling tree to high orders and to explain the intrinsic dynamic structures in detail. The insights gained from such analysis are not only valuable for understanding existing issues of mode coupling theory, but also shed light on how to improve MC for realistic systems.

B. Implication of Results. The purpose of this paper is not restricted to the East model but is aimed at a general understanding of mode coupling theory by demonstrating its construction, deficiency, and possible improvement. Here, we assess the predictive power of our analysis of the East model and explore the broader implication of the matrix formulation.

Our analytical results of the East model should be evaluated in the context of earlier studies on the same model. Because of the simplicity of the East model, several theorists have proposed exact mathematical procedures to predict its dynamics and long-time behavior. But most of these proposals are model-dependent and lack the generality of the matrix formulation. Because mode coupling theory is the standard tool for studying the dynamics of low temperature liquids, it is meaningful to apply the mode-coupling description to the simple East model and calibrate the underlying approximation systematically. Pitts and Anderson were the first to develop mode coupling closures to the east model and proposed simple and extended mode coupling expression.^{19,20} Using the matrix formulation, we are able to show that the results of extended mode-coupling (EMC) are almost indistinguishable from those of the basis set expansion method. The proposed long-time correction works well for $c = 0.2$, when the system exhibits strong slow relaxation. Thus, both EMC and the long-time MC closure successfully extend the validity of standard mode-coupling theory to lower temperatures.

The strength of the matrix formalism lies in its simple and transparent structure. To properly assess its predictive power, we must emphasize the differences between the East model and colloid systems. (1) Mode-coupling approximations belong to a class of mean-field approximation, which by definition work better if the interactions are more homogeneous. The East model has strong directional local dynamic constraints, which render mode coupling approximations less accurate. (2) Because of the unique coupling, the East model has a linear closure, whereas Gaussian factorization and quadratic closures are often used for colloids and liquids. (3) The East model has dynamic divergence at $c = 0$, whereas the hard-sphere colloid system has a finite transition density observed experimentally.¹⁷ More importantly, the length scale of dynamic domains in the East model diverge at the glass transition temperature. In real systems, the length scale does not grow to infinity. Consequently, the East model may very well represent a more difficult case than colloid suspensions and other realistic systems, for which the matrix formulation will be more reliable.

To support the above arguments, we recently applied the matrix formalism to calculate the dynamic scattering function of the hard-sphere colloidal system. The matrix formalism not only recovers the standard mode coupling memory kernel functions^{23,35} but also improves mode coupling transition predictions and provides a general factorization scheme for the slow functions of nonlinear modes. The standard MCT calculation predicts the glass transition at a reduced density of 0.52, which is significantly lower than the experimental value of 0.58.³¹ Our second-order MCT prediction gives 0.54 and the third order gives 0.55, which is probably the closest prediction to the observed colloidal glass transition point. Our prediction of the nonergodic parameter below the glass transition is also significantly improved. These encouraging results will be reported in a coming paper.²²

It is known that the standard MCT formalism is not adequate for describing the glass transition or the long-time behavior of low temperature liquids. However, combining complementary perspectives significantly extends the validity of standard MCT. For example, in the 2-D rotor paper, we used the hydrodynamic

basis set for the high-temperature phase and the spin wave basis set for the low-temperature phase.²¹ The connection between the two different basis sets remains a challenge. Another possibility is to use the low-temperature phase to guide high-order corrections. In a sense, the stretched exponential approximation is an example motivated by this possibility. Scaling relations combined with thermodynamics may very well provide the basis for understanding the low-temperature behavior and serve as the proper input for constructing high-order MCT closures. This paper and other recent publications from my group represent our effort along this direction.

Acknowledgment. The research is supported by the Petroleum Research Fund administrated by the American Chemical Society, the NSF Career Award(Che-0093210), and the Camille Dreyfus Teacher-Scholar Award.

Appendix A: Kinetic Matrix in the East Model

We construct a matrix \mathbb{L} to represent operator \mathbf{L} in the complete basis set of the East model introduced in section II. The detailed calculations on the matrix elements of \mathbf{L} are presented below on the basis of the fundamental rate equation, $\mathbf{L}A_1(i) = -A_1(i)n_{i+1}$. For an arbitrary mode $A_m(i_1i_2\cdots i_m)$, $\mathbf{L}A_m$ is given by a linear summation expression,

$$\begin{aligned} \mathbf{L}A_m(i_1i_2\cdots i_m) &= \sum_{k=1}^m \left[\prod_{j=1(\neq k)}^m A_1(i_j) \right] \mathbf{L}A_1(i_k) \\ &= - \sum_{k=1}^m \prod_{j=1(\neq k)}^m A_1(i_j) A_1(i_k) n_{ik+1} \end{aligned} \quad (\text{A1})$$

and the identity $n^s \equiv n$ ($s > 0$) is used to simplify this equation. Because the spin sequence is specified as ($i_1 < i_2 < \dots < i_m$) to avoid overcounting, only spins $i_{[k+1]}$ and $i_k + 1$ can be the same, giving

$$\begin{aligned} A_1(i_{k+1})n_{ik+1} &= \\ &\begin{cases} (1-c)A_1(i_k + 1) + \sqrt{c(1-c)} & \text{if } i_{[k+1]} = i_k + 1 \\ cA_1(i_{k+1}) + \sqrt{c(1-c)}A_1(i_k + 1)A_1(i_{k+1}) & \text{if } i_{[k+1]} > i_k + 1 \end{cases} \end{aligned} \quad (\text{A2})$$

Substituting eq A2 into eq A1, $\mathbf{L}A_m$ is simplified to

$$\begin{aligned} \mathbf{D}^+ A_m(i_1i_2\cdots i_m) &= -(m-p)c + p(1-c)A_m(i_1i_2\cdots i_m) - \\ &\sqrt{c(1-c)} \left[\sum_{\{k\}} A_{m-1}(i_1\cdots i_k i_{[k+2]}\cdots i_m) + \right. \\ &\left. \sum_{\{k'\}} A_{m+1}(i_1\cdots i_{k'}, [i_{k'} + 1], i_{[k'+1]}\cdots i_m) \right] \end{aligned} \quad (\text{A3})$$

where p spins satisfy $i_{[k+1]} = i_k + 1$ and are denoted by i_k and all the other spins are denoted by $i_{k'}$. All the matrix elements of \mathbf{L} are obtained by substituting eq A3 into the definition, $L_{m,m'} \equiv \langle f_{eq} A_m \mathbf{L} A_{m'} \rangle$, which leads to eqs 4–6.

Appendix B: Recursive Expressions for Slow Functions of Nonlinear Modes

In this appendix, we use the block matrix decomposition in the complete dynamic space to derive recursive expressions for the full and irreducible correlation functions.

1. Full Correlation Functions. Similar to $\hat{C}_1(z)$, the k th-order full correlation function $\hat{C}_k(z)$ is given by the (k, k) block

matrix element of $(z\mathbb{I} - \mathbb{L})^{-1}$. We rewrite eq 9 as

$$z\mathbb{I} - \mathbb{L} = \begin{bmatrix} z\mathbb{I} - \mathbb{L}_{k-1}^L & -(\mathbb{L}_{k-1,k}) & 0 \\ -(\mathbb{L}_{k-1,k})^T & z\mathbb{I} - \mathbb{L}_{k,k} & -(\mathbb{L}_{k,k+1}) \\ 0 & -(\mathbb{L}_{k,k+1})^T & z\mathbb{I} - \mathbb{L}_{k+1}^r \end{bmatrix} \quad (\text{B1})$$

where the submatrix coupling to lower order basis sets is defined as

$$\mathbb{L}_k^L = \begin{bmatrix} \mathbb{L}_{1,1} & \mathbb{L}_{1,2} & & & \\ \mathbb{L}_{2,1} & \ddots & \ddots & & \\ & \ddots & \ddots & \ddots & \\ & & \ddots & \mathbb{L}_{k-1,k} & \\ & & & \mathbb{L}_{k,k-1} & \mathbb{L}_{k,k} \end{bmatrix} \quad (\text{B2})$$

and the submatrix \mathbb{L}_k^r coupling to higher order basis sets is defined by eq 12. Off-diagonal row block matrices are denoted by $(\mathbb{L}_{k-1,k}) = [0 \ 0 \ \cdots \ \mathbb{L}_{k-1,k}]$, and the superscript T denotes the transpose matrix. We obtain the k th-order full correlation function,

$$\hat{C}_k(z) = [z\mathbb{I} + \Omega_k - \Omega_k^L(z) - \hat{M}_k(z)]^{-1} \quad (\text{B3})$$

where $\Omega_k^L(z)$ is the contribution from lower order basis sets,

$$\begin{aligned} \Omega_k^L(z) &= \mathbb{L}_{k,k-1} [z\mathbb{I} + \Omega_{k-1} - \Omega_{k-1}^L(z)]^{-1} \mathbb{L}_{k-1,k} \\ &= \mathbb{L}_{k,k-1} [z\mathbb{I} + \Omega_{k-1} - \mathbb{L}_{k-1,k-2} [z\mathbb{I} + \Omega_{k-2} - \\ &\quad \cdots]^{-1} \mathbb{L}_{k-2,k-1}]^{-1} \mathbb{L}_{k-1,k} \end{aligned} \quad (\text{B4})$$

Following eqs 13 and B4, an expression relating the reduced and full correlation function at the same order is

$$[\hat{C}_k^r(z)]^{-1} = \hat{C}_k^{-1}(z) + \Omega_k^L(z) \quad (\text{B5})$$

$$[\tau_k^r]^{-1} = \tau_k^{-1} + \Omega_k^L \quad (\text{B6})$$

where $\Omega_k^L \equiv \Omega_k^L(z=0)$. Using eq B5, we recast eq B3 into

$$\begin{aligned} \hat{C}_k(z) &= \left\{ z\mathbb{I} + \Omega_k - \Omega_k^L(z) - \mathbb{L}_{k,k+1} \left[\frac{\mathbb{I}}{\hat{C}_{k+1}(z)} + \right. \right. \\ &\quad \left. \left. \mathbb{L}_{k+1,k} \frac{\mathbb{I}}{z\mathbb{I} + \Omega_k - \Omega_k^L(z)} \mathbb{L}_{k,k+1} \right]^{-1} \mathbb{L}_{k+1,k} \right\}^{-1} \end{aligned} \quad (\text{B7})$$

Following a matrix formula, $[\mathbb{I} - \mathbb{A}(\mathbb{I} + \mathbb{B}\mathbb{A})^{-1}\mathbb{B}]^{-1} = \mathbb{I} + \mathbb{A}\mathbb{B}$, where the matrices $\mathbb{A}\mathbb{B}$ and $\mathbb{B}\mathbb{A}$ are invertible, eq B7 is simplified to a recursive expression for full correlation functions,

$$\begin{aligned} \hat{C}_k(z) &= \frac{\mathbb{I}}{z + \Omega_k - \Omega_k^L(z)} + \\ &\frac{\mathbb{I}}{z + \Omega_k - \Omega_k^L(z)} [\mathbb{L}_{k,k+1} \hat{C}_{k+1}(z) \mathbb{L}_{k+1,k}] \frac{\mathbb{I}}{z + \Omega_k - \Omega_k^L(z)} \end{aligned} \quad (\text{B8})$$

2. Irreducible Correlation Functions. We construct the k th-order irreducible correlation functions by omitting z dependence in kinetic contributions from all the basis sets lower than q_k , i.e., $\Omega_k^L(z)$ is replaced by $\Omega_k^L = \Omega_k^L(z=0)$ in eq B3,

$$\hat{C}_k^{\text{ir}}(z) = [z\mathbb{I} + \Omega_k - \Omega_k^L - \hat{M}_k(z)]^{-1} \quad (\text{B9})$$

Comparing eq B9 to eq 13, we obtain

$$[\hat{C}_k^r(z)]^{-1} = [\hat{C}_k^{\text{ir}}(z)]^{-1} + \Omega_k^L \quad (\text{B10})$$

which allows us to rewrite eq B9 as

$$\hat{C}_k^{\text{ir}}(z) = \left\{ z\mathbf{I} + \Omega_k - \Omega_k^L - \mathbf{L}_{k,k+1} \left[\frac{\mathbf{I}}{\hat{C}_{k+1}^{\text{ir}}(z)} + \mathbf{L}_{k+1,k} \frac{\mathbf{I}}{\Omega_k - \Omega_k^L} \mathbf{L}_{k,k+1} \right]^{-1} \mathbf{L}_{k+1,k} \right\}^{-1} \quad (\text{B11})$$

By applying the block matrix inversion method, we obtain a recursive expression for irreducible correlation functions,

$$\hat{C}_k^{\text{ir}}(z) = \left[z\mathbf{I} + \frac{(\Omega_k - \Omega_k^L) \mathbf{I} (\Omega_k - \Omega_k^L)}{\Omega_k - \Omega_k^L + \mathbf{L}_{k,k+1} \hat{C}_{k+1}^{\text{ir}}(z) \mathbf{L}_{k+1,k}} \right]^{-1} \quad (\text{B12})$$

Appendix C: Equivalence between Operator and Matrix Formalisms for the Irreducible Memory Kernel

In ref 18, Kawasaki introduced the irreducible operator,

$$\mathbf{L}_1 = \mathbf{L} - \mathbf{L}_0 = \mathbf{L} + \mathbf{L}q_1 \langle \Omega_1^{-1} \rangle f_{\text{eq}} q_1 \mathbf{L} \quad (\text{C1})$$

which is used to define the irreducible memory kernel

$$\begin{aligned} \hat{M}_1^{\text{ir}}(z) &= \langle f_{\text{eq}} q_1 \mathbf{L} \mathbf{Q}_1 [z\mathbf{I} - \mathbf{L}_1 \mathbf{Q}_1]^{-1} \mathbf{Q}_1 \mathbf{L} q_1 \rangle \\ &= \mathbf{L}_{1,2} \hat{C}_2^{\text{ir}}(z) \mathbf{L}_{2,1} \end{aligned} \quad (\text{C2})$$

$$\hat{C}_2^{\text{ir}}(z) = \langle f_{\text{eq}} q_2 [z\mathbf{I} - \mathbf{L}_1 \mathbf{Q}_1]^{-1} q_2 \rangle \quad (\text{C3})$$

The projection operators \mathbf{P}_k and \mathbf{Q}_k are defined in section IV.A. On the other hand, the operation expression for the second-order reduced correlation function is

$$\hat{C}_2^{\text{r}}(z) = \langle f_{\text{eq}} q_2 [z\mathbf{I} - \mathbf{L} \mathbf{Q}_1]^{-1} q_2 \rangle \quad (\text{C4})$$

By substituting eq C1 into eq C4, $\hat{C}_2^{\text{r}}(z)$ becomes

$$\begin{aligned} \hat{C}_2^{\text{r}}(z) &= \langle f_{\text{eq}} q_2 [(z\mathbf{I} - \mathbf{L}_1 \mathbf{Q}_1)^{-1} + \\ &\quad (z\mathbf{I} - \mathbf{L} \mathbf{Q}_1)^{-1} \mathbf{L}_0 \mathbf{Q}_1 (z\mathbf{I} - \mathbf{L}_1 \mathbf{Q}_1)^{-1}] q_2 \rangle \\ &= \hat{C}_2^{\text{ir}}(z) - \hat{C}_2^{\text{r}}(z) \Omega_2^L \hat{C}_2^{\text{ir}}(z) \end{aligned} \quad (\text{C5})$$

which is consistent with eq B10 and demonstrates the equivalence between our matrix formalism and Kawasaki's operator formalism for the first-order irreducible memory kernel.

To be consistent with $\hat{C}_2^{\text{ir}}(z)$ in eq C3, we define the k th-order irreducible correlation function as

$$\hat{C}_k^{\text{ir}}(z) = \langle f_{\text{eq}} q_k [z\mathbf{I} - \mathbf{L}_{k-1} \mathbf{Q}_{k-1}]^{-1} q_k \rangle \quad (\text{C6})$$

which arises from the operator definition, $\hat{C}_k^{\text{r}}(z) = \langle f_{\text{eq}} q_k [z\mathbf{I} -$

$\mathbf{L} \mathbf{Q}_{k-1}]^{-1} q_k \rangle$. In eq C6 we introduce the $(k - 1)$ th-order irreducible operator \mathbf{L}_{k-1} . The operator formalism in eq C5 gives

$$\hat{C}_k^{\text{r}}(z) = \left\langle f_{\text{eq}} q_k \left[\frac{1}{z\mathbf{I} - \mathbf{L}_{k-1} \mathbf{Q}_{k-1}} + \frac{1}{z\mathbf{I} - \mathbf{L} \mathbf{Q}_{k-1}} (\mathbf{L} - \mathbf{L}_{k-1}) \mathbf{Q}_{k-1} \frac{1}{z\mathbf{I} - \mathbf{L}_{k-1} \mathbf{Q}_{k-1}} \right] q_k \right\rangle \quad (\text{C7})$$

which is combined with eq B10 to give

$$\begin{aligned} \mathbf{L}_{k-1} &= \mathbf{L} - \mathbf{L} q_{k-1} \langle f_{\text{eq}} q_{k-1} [\mathbf{L} \sum_{m=1}^{k-1} \mathbf{P}_m]^{-1} q_{k-1} \rangle f_{\text{eq}} q_{k-1} \mathbf{L} \\ &= \mathbf{L} - \mathbf{L} q_{k-1} \langle \Omega_{k-1} - \Omega_{k-1}^L \rangle^{-1} \langle f_{\text{eq}} q_{k-1} \mathbf{L} \end{aligned} \quad (\text{C8})$$

References and Notes

- (1) Fredrickson, G. H.; Andersen, H. C. *Phys. Rev. Lett.* **1984**, *53*, 1244.
- (2) Fredrickson, G. H.; Andersen, H. C. *J. Chem. Phys.* **1985**, *83*, 5822.
- (3) Abrahams, E.; Palmer, R. G.; Stein, D. L.; Andersen, P. W. *Phys. Rev. Lett.* **1984**, *53*, 958.
- (4) Adam, G.; Gibbs, J. H. *J. Chem. Phys.* **1965**, *43*, 139.
- (5) Xia, X. Y.; Wolynes, P. G. *Proc. Natl. Acad. Sci. U.S.A.* **2000**, *97*, 2990.
- (6) Xia, X. Y.; Wolynes, P. G. *Phys. Rev. Lett.* **2001**, *86*, 5526.
- (7) Jackle, J.; Eisinger, S. *Z. Phys. B* **1991**, *84*, 11–124.
- (8) Eisinger, S.; Jackle, J. *J. Stat. Phys.* **1993**, *73*, 643.
- (9) Garrahan, J. P.; Chandler, D. *Phys. Rev. Lett.* **2002**, *89*, 035704.
- (10) Garrahan, J. P.; Chandler, D. *Proc. Natl. Acad. Sci. U.S.A.* **2003**, *100*, 9710.
- (11) Mauch, F.; Jackle, J. *Physica A* **1999**, *262*, 98.
- (12) Sollich, P.; Evans, M. R. *Phys. Rev. Lett.* **1999**, *83*, 3238.
- (13) Ritort, F.; Sollich, P. *Adv. Phys.* **2003**, *52*, 219.
- (14) Evans, M. R. *J. Phys.: Condens. Matter* **2002**, *14*, 1397.
- (15) Sollich, P.; Evans, M. R. *Phys. Rev. E* **2003**, *68*, 031504.
- (16) Aldous, D.; Diaconis, P. *J. Stat. Phys.* **2002**, *107*, 945.
- (17) Götze, W. In *Liquids, Freezing and Glass Transition*; Hansen, J. P., Levesque, D., Zinn-Justin, J., Eds.; North-Holland, Amsterdam, 1991.
- (18) Kawasaki, K. *Physica A* **1995**, *215*, 61.
- (19) Pitts, S. J.; Young, T.; Andersen, H. C. *J. Chem. Phys.* **2000**, *113*, 8671.
- (20) Pitts, S. J.; Andersen, H. C. *J. Chem. Phys.* **2001**, *114*, 1101
- (21) Witkoskie, J. B.; Wu, J. L.; Cao, J. S. *J. Chem. Phys.* **2004**, *120*, 5695.
- (22) Wu, J. L.; Cao, J. S., submitted.
- (23) Cichocki, B.; Hess, W. *Physica A* **1987**, *141*, 475.
- (24) Pitts, S. J.; Andersen, H. C. *J. Chem. Phys.* **2000**, *113*, 3945.
- (25) Kawasaki, K. *Ann. Phys.* **1970**, *61*, 1.
- (26) Schofield, J.; Lim, R.; Oppenheim, I. *Physica A* **1992**, *181*, 89.
- (27) Mori, H. *Prog. Theo. Phys.* **1965**, *34*, 399.
- (28) Wu, J. L.; Cao, J. S. *Phys. Rev. E* **2003**, *67*, 061116.
- (29) Schweizer, K. S.; Saltzman, E. J. *J. Chem. Phys.* **2003**, *119*, 1181.
- (30) Saltzman, E. J.; Schweizer, K. S. *J. Chem. Phys.* **2003**, *119*, 1197.
- (31) Szamel, G. *Phys. Rev. Lett.* **2003**, *90*, 228301.
- (32) Honnenberg, P. C.; Halperin, B. I. *Rev. Mod. Phys.* **1977**, *49*, 435.
- (33) Berthier, L.; Garrahan, J. P. *J. Chem. Phys.* **2003**, *119*, 4367.
- (34) Witkoskie, J. B.; Cao, J. S. *Phys. Rev. E*, in press.
- (35) Kawasaki, K. *J. Stat. Phys.* **1997**, *87*, 981.